The Propensity of α-Aminoisobutyric Acid (=2-Methylalanine; Aib) to Induce Helical Secondary Structure in an α-Heptapeptide: A Computational Study

by **Dongqi Wang***[a]), **Michael Friedmann**[a]), **Zrinka Gattin**[a]), **Bernhard Jaun**[b]), and **Wilfred F. van Gunsteren***[a])

[a]) Laboratory of Physical Chemistry, Swiss Federal Institute of Technology, ETH, CH-8093 Zürich (e-mail: wfvgn@igc.phys.chem.ethz.ch; wangd@igc.phys.chem.ethz.ch)

[b]) Laboratory of Organic Chemistry, Swiss Federal Institute of Technology, ETH, CH-8093 Zürich

We present a molecular-dynamics simulation study of an α-heptapeptide containing an α-aminoisobutyric acid (=2-methylalanine; Aib) residue, Val[1]-Ala[2]-Leu[3]-Aib[4]-Ile[5]-Met[6]-Phe[7], and a quantum-mechanical (QM) study of simplified models to investigate the propensity of the Aib residue to induce $3_{10}/\alpha$-helical conformation. For comparison, we have also performed simulations of three analogues of the peptide with the Aib residue being replaced by L-Ala, D-Ala, and Gly, respectively, which provide information on the subtitution effect at C(α) (two Me groups for Aib, one for L-Ala and D-Ala, and zero for Gly). Our simulations suggest that, in MeOH, the heptapeptide hardly folds into canonical helical conformations, but appears to populate multiple conformations, *i.e.*, C_7 and 3_{10}-helical ones, which is in agreement with results from the QM calculations and NMR experiments. The populations of these conformations depend on the polarity of the solvent. Our study confirms that a short peptide, though with the presence of an Aib residue in the middle of the chain, does not have to fold to an α-helical secondary structure. To generate a helical conformation for a linear peptide, several Aib residues should be present in the peptide, either sequentially or alternatively, to enhance the propensity of Aib-containing peptides towards the helical conformation. A correction of a few of the published NMR data is reported.

1. Introduction. – The properties of peptides that contain α-aminoisobutyric acid (=2-methylalanine; Aib) residues is an active area of research towards a better understanding of the folding behavior of peptides and the development of new folding entities [1–4]. Aib is a natural nonprotein amino acid, and occurs in polypeptide antibiotics found in fungi, molds, and spores [1][3].

Knowledge of the tendency of the Aib residue to promote helical conformation has been established based on crystallographical studies of peptides containing Aib residues, which reveal that the Aib residue is generally found in a 3_{10}-, α-, or mixed $3_{10}/\alpha$-helical conformation [1] with only a few exceptions where other conformations are adopted, such as the semiextended polyproline II (P_{II}) conformation. This is due to its unique structure, which differs from Ala and Gly by the presence of two Me groups at the C(α)-atom, *i.e.*, Ala and Aib are derived through single and double methylation of a Gly residue. A typical example of a peptide adopting an α-helix is Boc-Val-Ala-Leu-Aib-Val-Ala-Leu-(Val-Ala-Leu-Aib)$_2$-OMe [5] and an example of one adopting a 3_{10}-helix is Boc-Aib-Pro-Val-Aib-Val-Ala-Aib-Ala-Aib-Aib-OMe [6]. The conforma-

tional properties of α-peptides containing differently doubly substituted C(α)-atoms than Aib have also extensively been studied [7][8].

In a survey of the distribution of experimentally determined (ϕ,ψ) values (torsions centered on the N–C(α) and C(α)–C bonds in the polypeptide chain, resp., see *Fig. 1*) in 250 protein structures (resolution $\leq$2.0 Å) [9], the conformational space of the Aib residue is found to be confined to a very narrow region of left- and right-handed helical conformations, in contrast to the much broader distribution of Gly (in all four quadrants of the (ϕ,ψ) map), L-Ala, and D-Ala. The dramatic difference of allowed regions in their conformation spaces is due to the Me groups at the C(α)-atom [10]. Because of the double methylation, the C(α) in Aib is an achiral atom, without a preference for Aib to take either a left-handed or a right-handed conformation, and according to the available crystal structures, the two most populated regions are found at (ϕ,ψ) = ($-60^\circ \pm 20^\circ$, $-30^\circ \pm 20^\circ$) and (ϕ,ψ) = ($60^\circ \pm 20^\circ$, $30^\circ \pm 20^\circ$) in the *Ramachandran* map [4], with two troughs centered at (ϕ,ψ) = ($\pm 57^\circ$, $\pm 47^\circ$) [11].

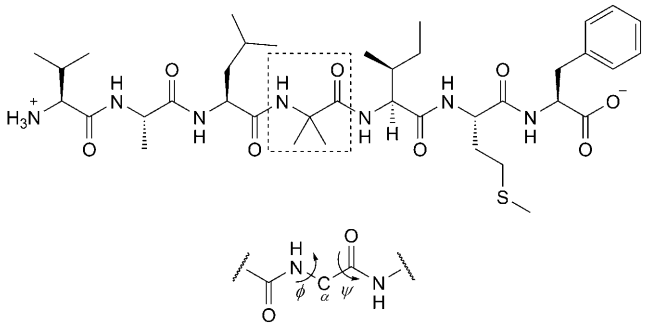

Fig. 1. *α-Peptide Val^1-Ala^2-Leu^3-Aib^4-Ile^5-Met^6-Phe^7*(= Pep_Aib) *and torsion angles (ϕ, ψ) used to characterize the backbone conformation of α-peptides.* The other three peptides differ from Pep_Aib by the replacement of the Aib^4 residue by L-Ala^4 (Pep_LAla), D-Ala^4 (Pep_DAla), and Gly^4 (Pep_Gly), respectively.

Hydrophobic interactions may induce helix nucleation [12] for sufficiently long polypeptides. For short-chain peptides or antibiotics, an alternative is to insert helix-inducing residues in the chain, such as residues with C(α) being geminally dimethylated. In addition, the narrow accessible conformational space of the Aib residue makes it suitable to produce rigid scaffolds and spacers [7][13]. For example, Aib was used in mixed α/β polypeptides [14] to generate new types of helical secondary structure.

But, how strong is this helix-inducing effect of an Aib residue? A major part of the available Aib-related peptide chemistry concentrates on Aib-rich peptides both experimentally [2] and theoretically [15–18]. Though a survey of a large set of helical structures does not give a clear correlation between the Aib content of a peptide and the deviation of its helical structure from the canonical helical secondary structure, we can not rule out the possibility that the formation of the helix actually results from the combined effect of all Aib residues in an Aib-rich peptide. For tripeptides with a single

Aib residue, helical structure is still observed [19][20], while there is no conclusive evidence that the helical folding in the presence of Aib residues is chain-length-independent. Meanwhile, for short peptides, the secondary structure observed in X-ray-crystallographic studies is not necessarily representative for the conformation of the peptide in solution due to the large difference between the two environments. Thus, spectroscopy, such as NMR, and computational studies are expected to provide direct evidence and reasonable explanations on the behavior of short peptides in solution, such as the relationship between the Aib content and the propensity to fold to a helical conformation, the solvent effect, *etc*.

Recently, an NMR investigation of an α-heptapeptide with one single Aib residue, Val[1]-Ala[2]-Leu[3]-**Aib[4]**-Ile[5]-Met[6]-Phe[7] (= Pep_Aib; see *Fig. 1*), has been reported which addresses this issue [21]. It was concluded that short α-peptides, though with an Aib residue, do not fold to a canonical helical structure in MeOH, which is considered to be a helix-stabilizing solvent, and that under the same conditions, α-peptides have a much lower propensity to fold to a helix compared to β-peptide analogues [22][23]. This conclusion is consistent with the prediction from a previous molecular-dynamics simulation [24] of a similar peptide, Val[1]-Gly[2]-Leu[3]-Aib[4]-Ile[5]-Met[6]-Phe[7], in both MeOH and H_2O that the α-peptide does not fold into a particular secondary structure. This suggests that molecular-dynamics simulations with the GROMOS force field can properly describe the folding behavior of peptides containing Aib residues.

The present study concerns the prototype α-heptapeptide Pep_Aib reported in the NMR study [21] with the aim to analyze the propensity of the Aib residue to induce folding to a helical conformation. This is a linear peptide with one Aib residue sitting in the middle of the chain and three other residues on each side. Taking advantage of the merits of molecular-dynamics simulation at the atomic level in conformational-space sampling [25–27], we hoped to obtain detailed information regarding the influence of the Aib residue on the conformation of peptides. For comparison, three other α-heptapeptides were chosen as model compounds to investigate the effect of Me groups at the C(α)-atom of the Aib residue in inducing helical structure. These peptides differ from Pep_Aib with the Aib[4] residue being replaced by L-Ala[4] (Pep_LAla), D-Ala[4] (Pep_DAla), or Gly[4] (Pep_Gly), respectively.

The current study differs from a previous one of a slightly different peptide [24] in a number of aspects. First, in [24] the second residue is denoted as Ala, but, in fact, a Gly residue was present as the second residue in the simulations. Second, because at the time the work reported in [24] was carried out, no NMR experimental data were available for the peptide, no comparison to experimental data could be done. As these became available [21], we decided to perform a more extended study of this peptide, including a variation of the Aib residue, a QM calculation and the effect of DMSO as solvent.

2. Computational Details. – *Molecular-Dynamics Simulations.* The four peptides and solvent were modelled with the GROMOS force field 53A6 [28]. The MeOH solvent molecules were modelled with a rigid three-site model [29]. Aliphatic CH_n groups ($n = 1-3$) were treated as united atoms, both in the solute and solvent. The terminal residues of the peptides, Val[1] on the N-terminus and Phe[7] on the C-terminus, were protonated. One of the model structures derived from NMR [21] was taken as the initial structure to start the molecular-dynamics simulations. The other three peptides were prepared by the mutation of the Aib residue in the NMR model structure. The systems Pep_Aib and Pep_LAla contained

3114 MeOH molecules and the systems Pep_D-Ala and Pep_Gly 3115. The initial length of the edges of the cubic periodic boxes was 5.97 nm.

A steepest-descent (SD) energy minimization was done to relax the solvent molecules after the solvation of the peptides. The solvated systems were then equilibrated for 1 ns, with the temp. being increased gradually from 60 K to 300 K. The initial velocities were assigned from a *Maxwell–Boltzmann* distribution at 60 K. During the equilibration phase, atom-positional restraints were used for the solute with the force constant being decreased from $2.4 \cdot 10^4$ kJ mol^{-1} nm^{-2} to 0 within 800 ps. The final coordinates and velocities of the equilibration phase were then used to start the sampling. Rectangular periodic boundary conditions [30][31] were applied in all molecular-dynamics simulations. The leap-frog algorithm was used to integrate *Newton*'s equations of motion with a time step of 2 fs. All bond lengths and the MeOH bond angle were constrained to their ideal values by means of the procedure SHAKE [32] with a geometric precision of 10^{-4}. Long-range electrostatic interactions were handled with a twin-range cutoff scheme [30][31] with cutoff radii of 0.8 nm (interactions updated every time step) and 1.4 nm (interactions updated every five time steps). The mean effect of omitted electrostatic interactions beyond the long-range cutoff distance (1.4 nm) was accounted for by the inclusion of a *Barker–Watts* reaction-field force [33][34] based on a permittivity of 18 for MeOH [29]. The weak-coupling method [35] was used for keeping the temp. (300 K) and pressure (1 atm) constant, by means of coupling times τ_T 0.1 ps. and τ_P 0.5 ps and an isothermal compressibility of $1.6 \cdot 10^{-3}$ kJ^{-1} mol nm^3 [29]. Trajectory coordinates were saved every 0.5 ps for analysis.

The analysis of trajectories was similar to that in previous work [36]. Atomic positional root-mean-square differences (RMSD) were calculated for MD trajectory structures with respect to the NMR model structure [21]. The criterion used in the H-bond analysis was 0.25 nm as upper bound of the H$\cdots$A (A = acceptor) distance and 135° as lower bound of the D$\cdots$H$\cdots$A angle (D = donor). A conformational-cluster analysis [37] was carried out on the combined trajectories of the peptides with structures at 10 ps intervals, respectively, by using as backbone (residues 2–6) the RMSD similarity criterion 0.08 nm. The available H–H distance bounds, which were derived from measured NOE cross-peak intensities [21], were compared to averages over the 100 ns trajectories, calculated as $\langle r^{-6} \rangle^{-1/6}$. The H–H distances involving aliphatic H-atoms were calculated by defining virtual (CH_1), prochiral ('stereospecific' CH_2), and pseudo (Me and 'non-stereospecific' CH_2) atomic positions, and the distance bounds for the latter were modified to include pseudo-atom distance-bound corrections [38]. ^3J-Coupling constants were obtained for the simulated and NMR-model structures with the *Karplus* relation [39][40] $^3J(H_N,H_{\alpha/\beta}) = a \cos^2\theta + b \cos\theta + c$, where θ is the dihedral angle between the planes defined by the atoms (H, N, C(α)) and the atoms (N, C(α), H(α) (= H–C(α))). The parameters a, b, c were 6.4, −1.4, and 1.9 Hz, resp. [41].

The experimentally obtained data [21], 66 H–H NOE distance bounds and 4 $^3J(H_N,H_{\alpha/\beta})$ coupling constants, are specified in Tables S1 and S2 of the Supporting Information[1]), together with the corresponding distance and ^3J-value averages obtained from the MD simulations and the set of NMR model structures, which had been obtained [21] by single-structure refinement by means of simulated temperature annealing with the program XPLOR.

To analyze the solvent influence on the ϕ/ψ distribution of the Aib residue, we also performed MD simulations of Pep_Aib in DMSO and H_2O. The setup of these two simulations was the same as that of the ones in MeOH described above. The solvent-specific parameters used in these two simulations are given in [42][43]. For the permittivities, we used the values of 46.6 for DMSO [42] and 61.0 for H_2O [44]. An isothermal compressibility of $4.575 \cdot 10^{-4}$ kJ^{-1} mol nm^3 was used for both solvents. Details of these simulations will be published elsewhere.

QM Calculations. The potential energy surfaces with respect to the ϕ and ψ torsional angles of the four amino acid residues Aib, L-Ala, D-Ala, and Gly were investigated with the QM method. The structures of the model compounds are shown in *Fig. 2*. Model QM_Aib (*N*-acetyl-*N*′-methyl-α-

---

[1]) Supporting Information is available free of charge upon request from *W. F. v. F.* or *D. W.* (wfvgn@igc.phys.chem.ethz.ch or wangd@igc.phys.chem.ethz.ch), *i.e.*, experimentally determined and calculated ^3J-coupling constants, NOE distance bounds and violations, and a *Ramachandran* map for the 20 NMR model structures.

aminoisobutyramide = 2-(acetylamino)-2,*N*-dimethylpropanamide = N^2-acetyl-N^1,2-dimethylalaninamide) is a prototype compound used in previous work of interest on the conformational states of the Aib residue, both experimentally [45] and theoretically [46–48]. The first four models differ in the presence of a Me group at the C(α)-atom. The calculations showed that the capping C=O and NH groups may form a seven-membered-ring (C7) H-bond in our simplified models, thus a fifth model (QM_Aib′), with the capping Ac group being replaced by its isoelectronic analogue, a MeC=CH_2 group, was prepared to avoid the conformational restriction that is created by the C7 H-bond. The hybrid density-functional method B3LYP [49][50] was used in combination with a double ζ quality basis set, 6-31G(d) [51], for the treatment of C-, N-, O-, and H-atoms. The B3LYP functional, which contains 20% HF exchange, has been used with great success for the prediction of geometry, relative energy, and electronic structure of the ground-state in a wide range of molecular systems [52][53]. Although showing a tendency to underestimate H-bond strength, it does yield good relative H-bond energies with small errors and thus outperforms many other functionals [53]. Unless stated otherwise, all QM results reported here are from the calculations at the level of B3LYP/6-31G(d) with the Gaussian03 package [54].

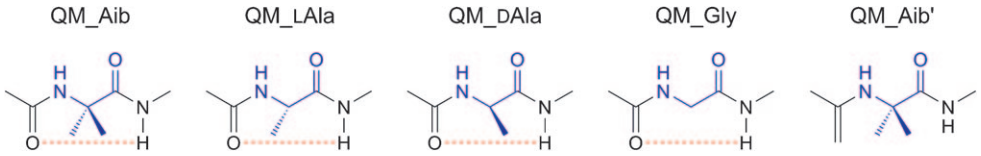

Fig. 2. *The model compounds used in the QM calculations for the investigation of the potential-energy surfaces with respect to ϕ and ψ.* Residues in blue, capping groups (Ac, $MeCCH_2$ and NHMe) in black, the seven-membered-ring H-bond in red.

3. Results and Discussion. – 3.1. *Potential-Energy Surface with Respect to ϕ and ψ from QM Calculations.* In *Fig. 3*, we plot the energy landscape in the *Ramachandran* map based on the calculations of the model compounds (see *Fig. 2*) in the gas phase. As seen in *Fig. 3*, the allowed conformational states in the conformational space of the model compound QM_Aib are predicted in the regions of the C_7 (centered at $(\phi,\psi) = (-73°, 60°)$), C'_7 (centered at $(\phi,\psi) = (73°, -58°)$), right-handed (centered at $(\phi,\psi) = (-67°, -26°)$; denoted as $Helix^R$), and left-handed (centered at $(\phi,\psi) = (67°, 26°)$; denoted as $Helix^L$) helices. As seen in *Table 1*, after taking into account the zero-point energy (*ZPE*) correction, the C_7 and C'_7 conformations are marginally more stable than the C_5 conformation, while the helical conformations, both left- and right-handed, are 10.6 kJ/mol above the C_5 one. This is consistent with the conclusions from previous experimental [45] and theoretical [48] work that both C_5 and C_7 conformations occur for Aib residues. Though a survey of the crystal structures of the peptides containing at least one Aib residue displays an overwhelming preference for the $3_{10}/\alpha$ helical conformation, C_7 and C'_7 conformations do exist in nonpolar solvents [45]. Ac-Aib-NHMe may take the α-helical conformation in the solid state, while it also populates the C_7 and C_5 conformations in nonpolar solvents according to IR spectroscopic studies in CCl_4 [45].

We note that in a recent DFT study [55] of diastereoisomeric trialanine peptides that are protected by an Ac group at the N-terminus and by a carboxamide at the C-terminus, conformations with a larger dipole moment generally gain more stabilization than those with a smaller dipole moment when taking into account the solvation free energy in H_2O. In the present study, the two helical conformations have larger dipole

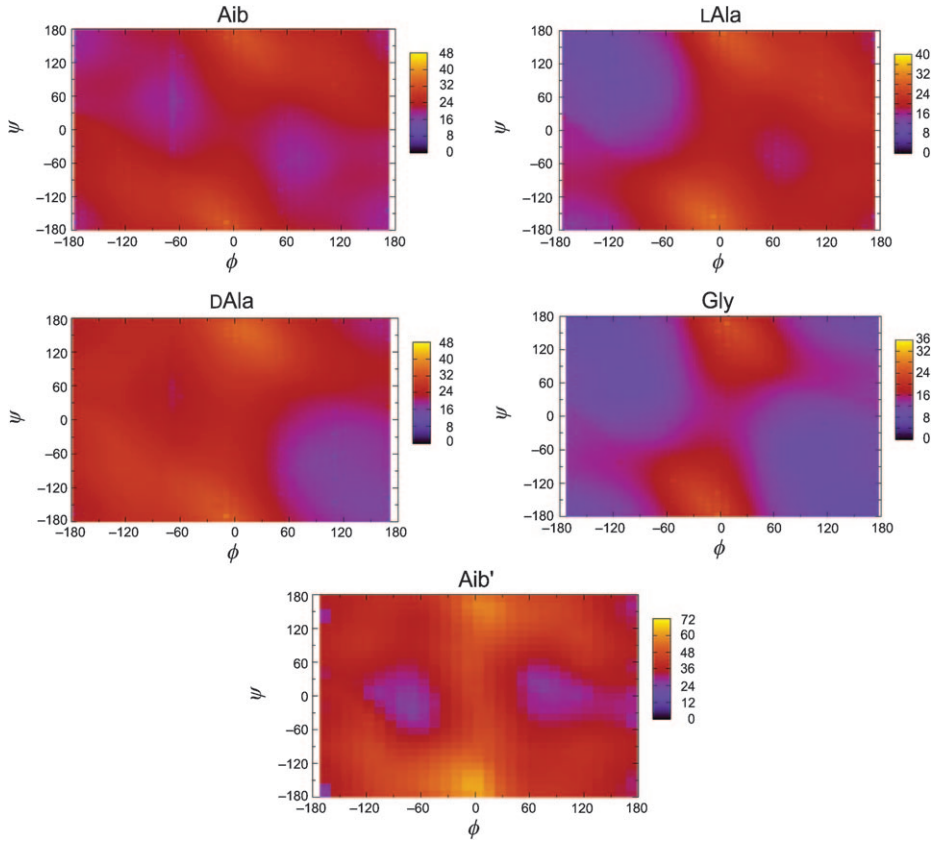

Fig. 3. *The allowed regions in conformational space of Aib,* L*-Ala,* D*-Ala, Gly, and Aib′ fragments* (see *Fig. 2*) *as obtained from density-functional calculations.* The energy is given as a color scale in kJ mol^{-1}.

moments than the other three (see *Table 1*), and so the helical conformations are expected to be stabilized more than the C_7 ones after being solvated.

In the C_7 conformation, a seven-membered-ring (C7) H-bond forms and brings substantial stabilization, as in the DFT study of two diastereoisomeric trialanine

Table 1. *Characterization of the Five Minima of Model QM_Aib*

	C_5	C_7	C'_7	Helix^L	Helix^R
ΔE [kJ mol^{-1}]	0.0	– 1.4	– 1.5	11.0	11.0
ΔZPE [kJ mol^{-1}]	0.0	0.6	0.8	– 0.4	– 0.4
μ [Debye]	3.6	3.3	3.3	5.5	5.5
ϕ	– 180.0°	– 72.8°	73.4°	66.7°	– 66.7°
ψ	– 179.9°	59.6°	– 58.0°	26.1°	– 26.0°
O···H [nm]	0.202	0.189	0.189	–	–
O···H–N	112.8°	152°.1	152.9°	–	–

peptides with L- and D-Ala in the middle, respectively [55]. This conformation is considered to be less favorable in polypeptides due to their intrinsic constraints. To minimize the influence of the C7 H-bonding, we have also investigated the energy landscape of a modified model, QM_Aib′, in which the C=O group is replaced by a $C{=}CH_2$ group. After the Ac group is replaced by a 1-methylvinyl group, the C7 H-bond is disrupted, and the global minima in the (ϕ,ψ) space were found with a right-handed $(\phi,\psi) = (-71^\circ, -30^\circ)$, and a left-handed $(\phi,\psi) = (71^\circ, 30^\circ)$ helical conformation. This suggests that the intramolecular seven-membered-ring H-bond is the determining force in the formation of the C_7 and C'_7 conformations.

A previous theoretical study based on molecular-orbital theory has argued that the theoretical prediction of the formation of a C_7 conformation may be due to an overestimation of the stabilization energy coming from the intramolecular H-bond [11]. This accentuates the importance of using advanced QM methods and a balanced basis set that are adequate for the description of non-bond interactions. In our present work, we use a generalized-gradient-approximation (GGA) functional (B3LYP) which takes into account electronic correlation. Though less suitable for the treatment of dispersion effects, the B3LYP functional has been suggested [52][53] to be an appropriate choice in the study of a wide range of molecular systems towards the reasonable description of relative conformational energies. Thus, when concerning the possible conformations of short peptides in the gas phase, the possible presence of C_7 and C'_7 conformations should not be readily excluded. For a short and flexible linear molecule, it is conceivable that it may take different conformations in the crystalline state, in the condensed phase, and the gas phase. In the crystalline state, additional forces coming from the crystal matrix, *i.e.*, packing effects, may overtake the intramolecular H-bonding force and dominate the conformation of the molecule. In contrast, in the gas phase and liquid phase, the molecule is not fixed in a matrix and has much larger motional freedom, thus the intramolecular forces, in collaboration with the non-bond interactions with the molecules in the surroundings (solute and solvent), may dominate. Indeed, the experiments on a dipeptide [45], which gave different conformations in an X-ray crystallographic study and in an IR spectroscopic study in CCl_4, clearly support this statement.

In case of models QM_LAla, QM_DAla, and QM_Gly, the former two display strong stereoselectivity due to the chirality of C(α) and take either one of the two mirror-image conformations depending on the chirality of C(α), while the latter shows a much wider allowed region, as expected.

3.2. *Comparison with NOE Atom–Atom Distance Bounds Derived from Experiment.* We calculated the NOE-distance-bound violations of the simulated geometries by referring to the NMR experimental data [21]. The results are plotted in *Fig. 4*. Amongst the 66 NOE-distance bounds determined from experiment [21], most of the NOE-distance-bound violations are below 0.1 nm, except for the six values that are collected in *Table 2*. Most of the NOE-distance bounds that display violations are in the range of weak to very weak intensity, except for the one between the H-atom pair Ile^5:HN-Met^6:HN (0.28 nm, NOE Nr. 45) which is close to the C-terminus of the peptide. The NOE-distance bounds involving the Aib^4 residue are well reproduced in the MD simulation. The simulated value for the H-atom pair Met^6:HN-Leu^3:H_α (0.72 nm) is much longer than the experimental NOE-distance bound (0.32 nm),

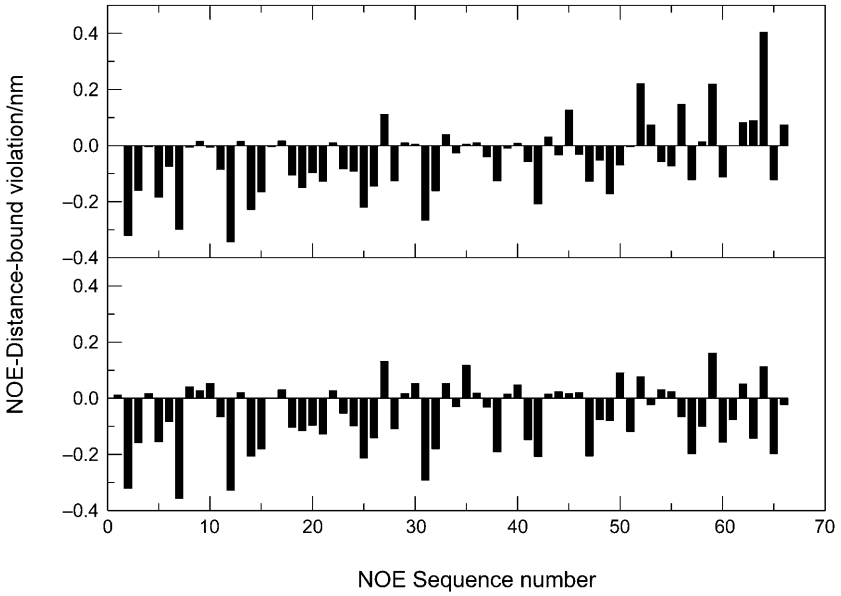

Fig. 4. *Average NOE-distance-bound violations in Pep_Aib.* Upper panel: MD simulation; lower panel: 20 NMR model structures [21].

Table 2. *Six NOE Distance Bounds and* r^{-6} *Averaged Distances from MD Simulation* [nm] *That Are Larger than 0.1 nm.* For details, see Table S2 in the Supporting Information[1]).

NOE No.	H-Atom pair[a])	Bound	MD	NOE Intensity [21]
27	$Val^1:H_\beta$-$Ala^2:H_\alpha$	0.36	0.47	weak
45	$Ile5:HN$-$Met^6:HN$	0.28	0.41	medium
52	$Leu^3:H_\alpha$-$Met^6:H_\gamma$*	0.46	0.68	very weak
56	$Leu^3:H_\beta$*-$Met^6:HN$	0.50	0.65	very weak
59	$Ile^5:H_\beta$-$Ala^2:HN$	0.43	0.65	weak
64	$Met^6:HN$-$Leu^3:H_\alpha$	0.32	0.72	weak

[a]) $H_\alpha = H-C(\alpha)$, $H_\beta = H-C(\beta)$, $H_\gamma = H-C(\gamma)$; the asterisk (*) means that a pseudoatom was used for the calculation, and the distance bound was adapted [38].

indicating that the simulation predicts a conformational ensemble in which the most-populated, rather extended conformation (*cf.* below, *Fig. 10,a*) is only 27% populated, while the third cluster (*cf.* below, *Fig. 10,c*) is more compact and 10% populated. The mentioned NOE violation indicates that the MD trajectory generated with the GROMOS force field slightly underestimates the helix propensity, as was observed earlier for a β-9-peptide in MeOH [56].

The complete set of 66 NOE bounds derived from experiment [21] and the r^{-6} averaged distances are specified in Table S3 of the Supporting Information[1]). Compared to the 68 NOE distances derived from experiment as reported in Table 2

of [21], one bound was corrected (Nr. 18) from 0.24 to 0.25 nm, one atom pair was corrected (Nr. 67) by changing H(α) to H(β) in residue 4, and two atom pairs were omitted (Nrs. 46 and 59). They turned out to be incorrectly reported in [21] due to errors occurring during conversion of the NOE bounds table as used in the structure determination to Table 2 of [21].

3.3. *Comparison to Measured* ^{3}J-*Coupling Constants.* Experimentally, there are four ^3J-coupling constants ($^3J(H_N,H_\alpha)$) available for model compound Pep_Aib that are assigned to Ala^2 (6.85 Hz), Leu^3 (6.24 Hz), Ile^5 (7.70 Hz), and Met^6 (7.83 Hz) [21], representing the residues on both sides of the Aib^4 residue. Using the *Karplus* relation, we calculated and averaged the ^3J values from the series of geometries obtained from the molecular-dynamics simulations. The results are shown in *Fig. 5*. The largest deviation is found for Leu^3. The calculated value for $^3J(H_N,H_\alpha)$ of Leu^3 is 7.36 Hz, larger than the experimentally measured value of 6.24 Hz. However, the accuracy of the *Karplus* relation is *ca.* 1 Hz. Thus, the good agreement between the experimentally determined data and the values calculated from the simulation indicates that most of the conformations that contribute to the ^3J-coupling constants determined experimentally have been sampled in our simulation.

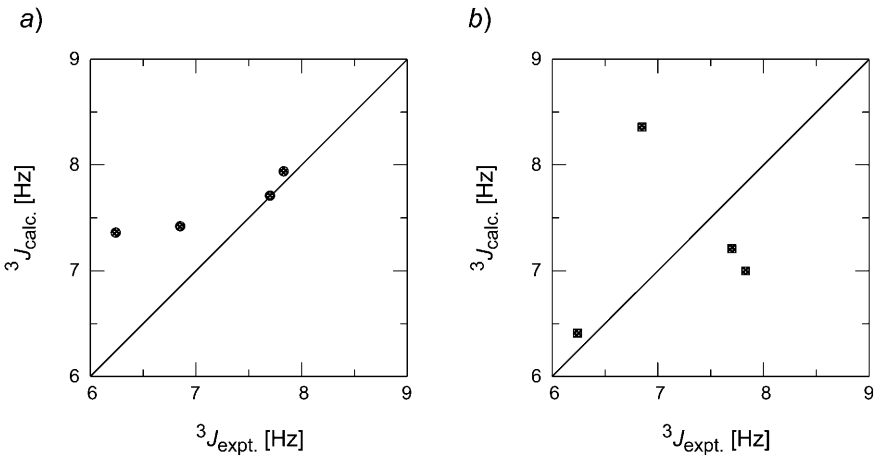

Fig. 5. *Average* ^{3}J-*coupling constants. a*) MD Simulation. *b*) 20 NMR Model structures [21].

3.4. *Structural Characterization of the Peptides. Root-Mean-Square Deviation* (RMSD). We took one of the bundle of NMR model structures which was calculated to have the lowest energy by XPLOR as the reference structure for the calculation of the atom-positional RMSD of the peptide-backbone atoms (N, C(α), and C). The results are plotted in *Fig. 6*. Substantial deviations are found in all model compounds, suggesting a more extended conformational space sampled in the simulations. In the simulation of Pep_Aib, half of the trajectory deviates less than 0.2 nm from the reference structure, while another half has a RMSD larger than 0.2 nm. This indicates that a much bigger conformational space than spanned by the NMR model structures has been sampled.

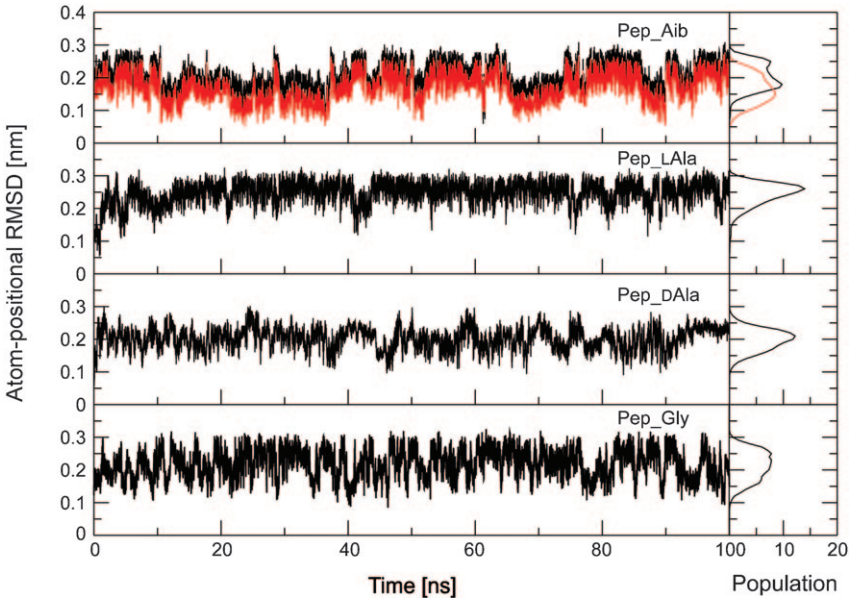

Fig. 6. *Atom-positional RMSD of the trajectory structures from the NMR model structure* [21] *for the backbone atoms* (N, C(β), C(α), C) *of residues 2–6 as a function of simulation time.* The reference structures used for the other three peptides have the same backbone conformation as the NMR model structure. The red line in the upper panel is from the calculation of the RMSD with a second NMR model structure [21] as reference structure which has the Aib torsion angles $(\phi,\psi) = (75°, -31°)$.

When the Aib residue is replaced by an L-Ala or a D-Ala residue, the trajectory in the 100-ns simulation populates a more narrow region with an average RMSD of 0.25 nm (L-Ala) or 0.20 nm (D-Ala) with respect to the NMR model structure. In the simulation of Pep_Gly, the distribution becomes broader. Therefore, the conformational space that the simulation of Pep_Aib has visited is closer to the NMR model structure than that in the simulations of the other three peptides. As the backbone fold of the NMR model structure is a right-handed helix (for Aib, $(\phi,\psi) = (-54.5°, -57.3°)$), the smaller the RMSD, the closer the structure is to this helical conformation. This suggests that when an Aib residue is inserted in the peptide, a driving force towards a helical fold is indeed introduced into the peptide.

Hydrogen Bond. The GROMOS force fields do not contain a special term in the interaction function to mimic H-bonding but describe this through a balance between the *Coulomb* and *van der Waals* attraction and repulsion, which has been tested in a large number of investigations of small peptides and protein molecules. Thus, it is reasonable to use the time evolution of H-bonds as an indicator of the stability of a conformation that has been visited in the MD simulations. We only monitored the occurrence of major H-bonds (with a presence larger than 5%) in the 100 ns simulations. The results are shown in *Fig. 7.* In the simulation of Pep_Aib (*Fig. 7,a*), the major H-bond is formed between Ile^5:HN and Leu^3:O, with a population of 45% of the whole trajectory. It closes a seven-membered ring. The second major H-bond is Aib^4:HN-Ala^2:O (9%). Both H-bonds are formed with the pattern $i+2 \rightarrow i$. Previous

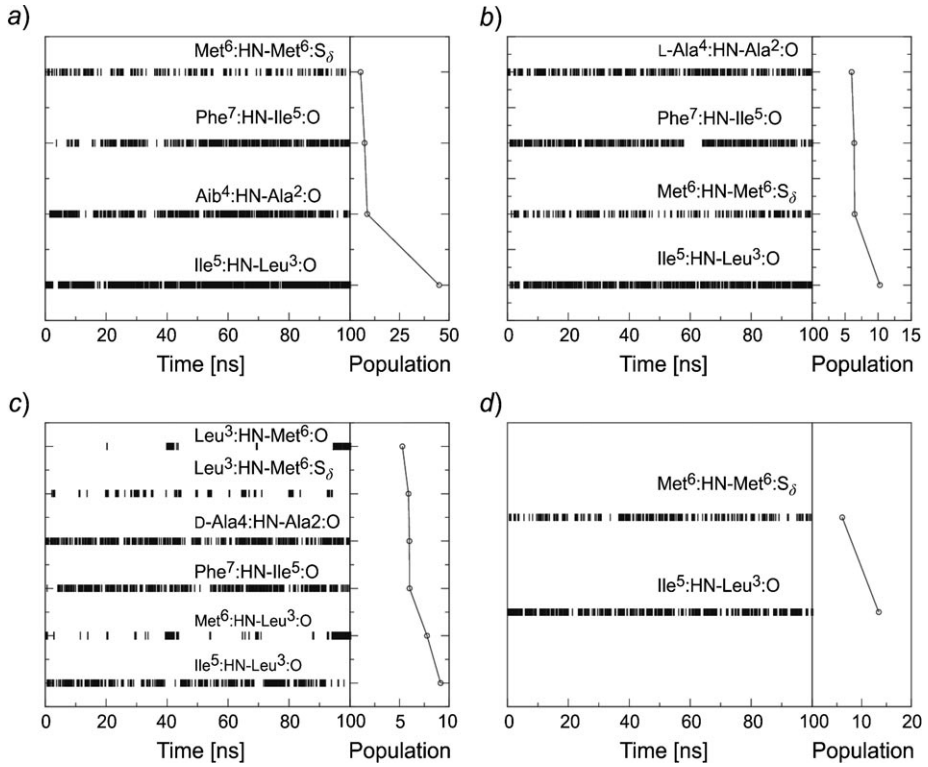

Fig. 7. *Occurrence of H-bonds with a population larger than 5% in the four simulations of the four peptides:* a) *Pep_Aib,* b) *Pep_*L*Ala,* c) *Pep_*D*Ala, and* d) *Pep_Gly* ($S_\delta = S(\delta)$)

studies [57] have suggested that the H-bond pattern in a 3_{10}-helix is $i+3 \rightarrow i$, while it is $i+4 \rightarrow i$ in an α-helix. We do observe such H-bonds in the MD simulations, for example, Ile^5:HN-Ala^2:O (4.5%), Met^6:HN-Leu^3:O (1.0%), Phe^7:HN-Aib^4:O (0.5%), and Aib^4:HN-Val^1:O (0.1%). These H-bonds show a low presence compared to the $i+2 \rightarrow i$ ones. This suggests that, in the heptapeptide, the Aib residue does show the propensity to induce a local helical conformation, but that this is not sufficient to make it the dominant conformation of the peptide.

In the simulations of Pep_LAla, Pep_DAla, and Pep_Gly (*Fig. 7,b–d*), though the H-bond Ile^5:HN-Leu^3:O still appears as the major H-bond, its presence is calculated to be only *ca.* 10%, which is much less than that in the simulation of Pep_Aib. Moreover, during more than half of the simulation time, there is no H-bond at all (see *Fig. 8*). This indicates that the simulations of Pep_LAla, Pep_DAla, and Pep_Gly have sampled a conformational space with much more extended protein-backbone structure than that of Pep_Aib.

Conformational Clustering. Conformational-clustering analysis [37] was done to characterize the conformational ensemble generated in the MD simulations. In the analysis, we grouped the structures in the trajectory into one cluster if their backbone (residues 2–6) RMSDs from each other are smaller than 0.08 nm. To compare the

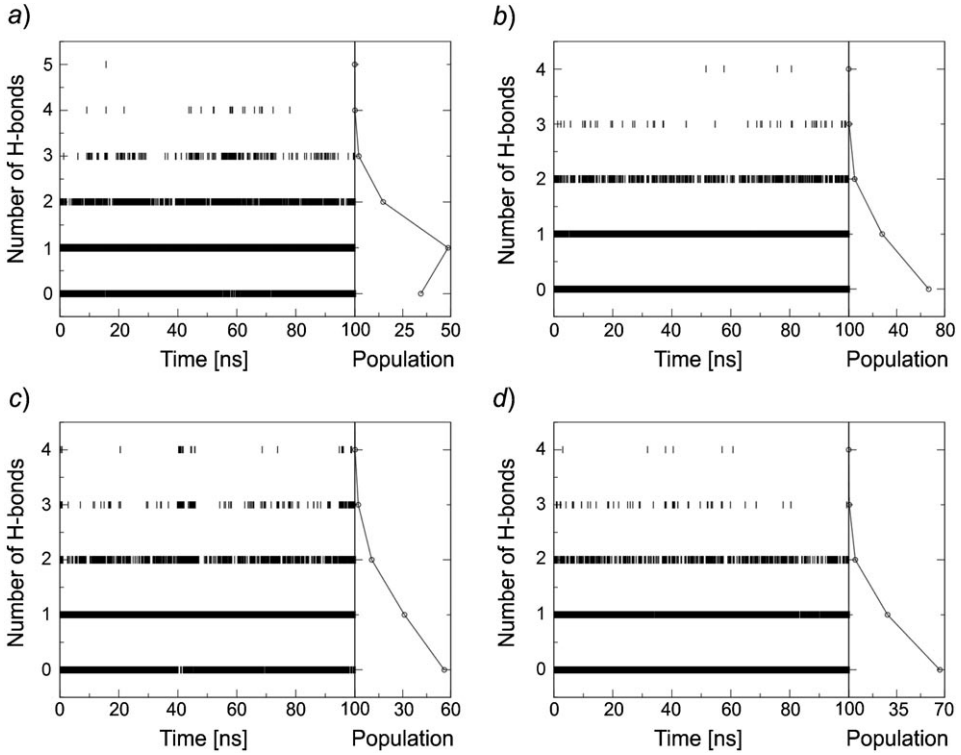

Fig. 8. *The number of H-bonds as a function of time in the simulations of the four peptides:* a) *Pep_Aib,* b) *Pep_*L*Ala,* c) *Pep_*D*Ala, and* d) *Pep_Gly*

propensity of the Aib residue to induce helicity with that of Ala and Gly residues, we combined the trajectory of Pep_Aib with that of each of the three simulations of the other three peptides with a time interval of 10 ps, thus using 10000 structures from each trajectory. The populations of the clusters are shown in *Fig. 9*, and representative members of the major cluster in each analysis are shown in *Fig. 10*.

As seen in *Fig. 9*, in the combined conformational-clustering analysis of the trajectories of Pep_Aib and Pep_LAla, the cluster with the largest population has almost equal contributions from both trajectories. In this cluster (*Fig. 10*,*a*), there is a seven-membered-ring H-bond between Ile^5:HN and Leu^3:O, suggesting that both L-Ala and Aib can bridge a H-bond donor and acceptor to form this type of H-bond. The second most populated cluster, which contains mainly Pep_LAla structures, is more extended compared to the largest and the third-largest clusters. The third-largest cluster is largely composed of structures of the trajectory of Pep_Aib, and the seven-membered-ring H-bond is also observed. Thus, the segment containing the Aib residue has a stronger propensity to bend than that with an L-Ala residue.

D-Amino acid residues favor a left-handed conformation, in contrast to L-amino acid residues, and when present in a peptide chain of L-amino acid residues, they

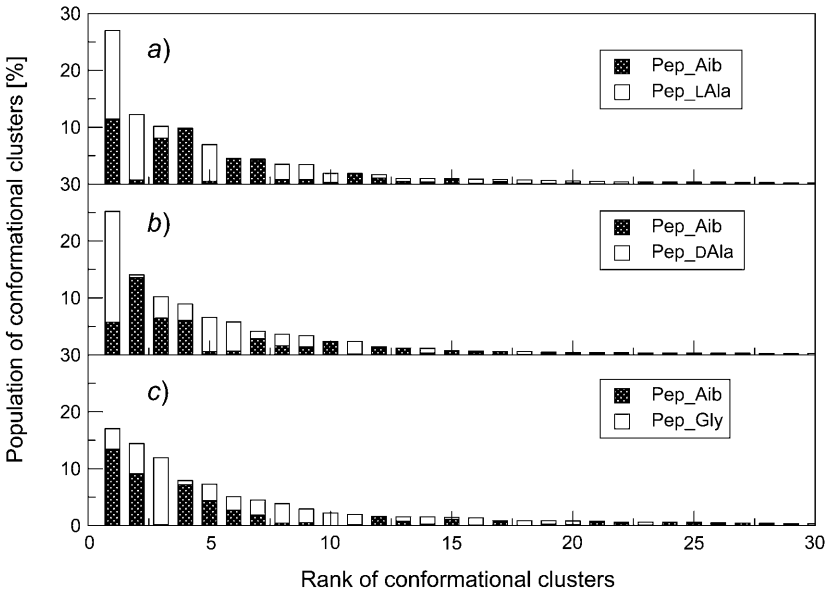

Fig. 9. *Conformational-clustering analysis over the 100-ns trajectories of Pep_Aib and each of the three other peptides* (atom-positional RMSD within 0.08 nm for backbone N, C(β), C(α), and C-atoms of residues 2–6)

destabilize or terminate a helical conformation [3]. In the analysis of the trajectories of Pep_Aib and Pep_DAla, the central structure of the cluster with the largest population displays a different feature compared to the case of Pep_LAla. The seven-membered-ring H-bond is disrupted. The cluster with the second largest population, which is composed mainly of structures from the trajectory of Pep_Aib, shows the formation of the seven-membered-ring H-bond between Ile^5:HN and Leu^3:O. Thus, Aib favors the C7 H-bond more than D-Ala does.

Gly often appears in a β-turn [1][58][59] to induce chain reversal [3]. This propensity of Gly was reproduced in our simulations. As seen in *Fig. 9,c*, the first two most-populated clusters, which show the C7 H-bond, have only a minor contribution from the trajectory of Pep_Gly. In contrast, the third largest cluster, which is almost completely composed of structures of Pep_Gly, has a H-bond between Gly^6:HN and Leu^3:O (0.213 nm) closing a ten-membered ring, thus showing a tight two-residue β-turn (*Fig. 10,i*), as proposed in previous studies [60–62].

In summary, the conformational-clustering analysis of the trajectories suggests a stronger propensity of the Aib residue to bend, and the tendency of an L-Ala residue to adopt an extended conformation. Gly shows a preference to appear in a β-turn.

(ϕ,ψ) Space (*Ramachandran* Plot). The *Ramachandran* plots are shown for all nonterminal residues (residues 2–6) in the four peptides in *Fig. 11*. In the case of Pep_Aib, similar to what we observed in the QM results, the sampling has covered the regions of C_7 ((ϕ,ψ) = ($-73°$, 37°)), C'_7 ((ϕ,ψ) = (66°, $-43°$)), right-handed ((ϕ,ψ) = ($-57°$, $-45°$)), and left-handed ((ϕ,ψ) = (61°, 34°)) helical conformations with a

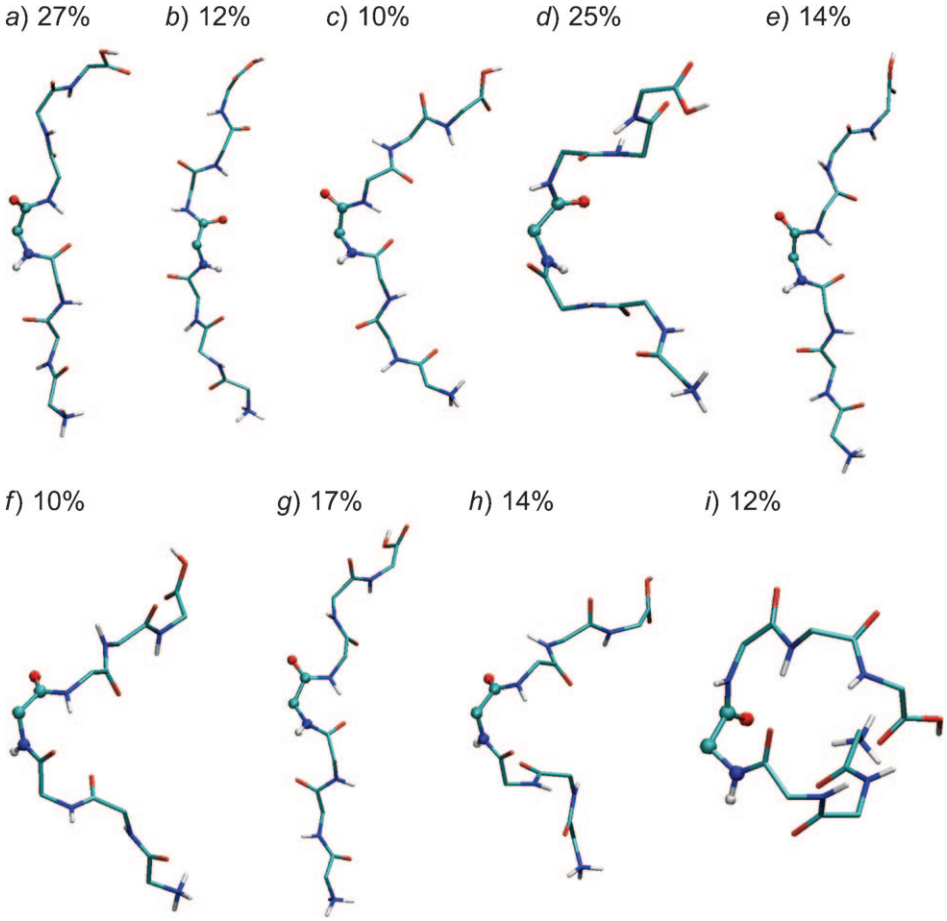

Fig. 10. *The central structures of the three major conformational clusters in the analysis over the 100-ns trajectories of Pep_Aib and each of the three other peptides* (see also *Fig. 9*; only the backbone is shown; the fourth residue (Aib[4], L-Ala[4], D-Ala[4], and Gly[4]) is shown in ball-and-stick). *a*)–*c*) Combined clustering of Pep_Aib and Pep_LAla. *d*)–*f*) Combined clustering of Pep_Aib and Pep_DAla. *g*)–*i*) Combined clustering of Pep_Aib and Pep_Gly.

minor population at the bridge region ($\psi = 0°$). Experimentally, the 20 NMR model structures calculated with X-PLOR are found almost equally in the regions that are characterized as Helix^R, Helix^L, and C'_7 conformations (see Fig. S1 in the Supporting Information[1])). Although our simulations show a higher population of the C'_7 conformation, the helical conformations do appear significantly in the trajectory. Meanwhile, the simulations predict that a transition among the four states is possible at 300 K, which is in line with the NMR measurement.

The folding behavior of oligomers does depend on the environment (solvent effect), the chain length, and the composition of the peptide [48]. We note that MeOH was used as solvent in our simulations, which is different from that in an experimental

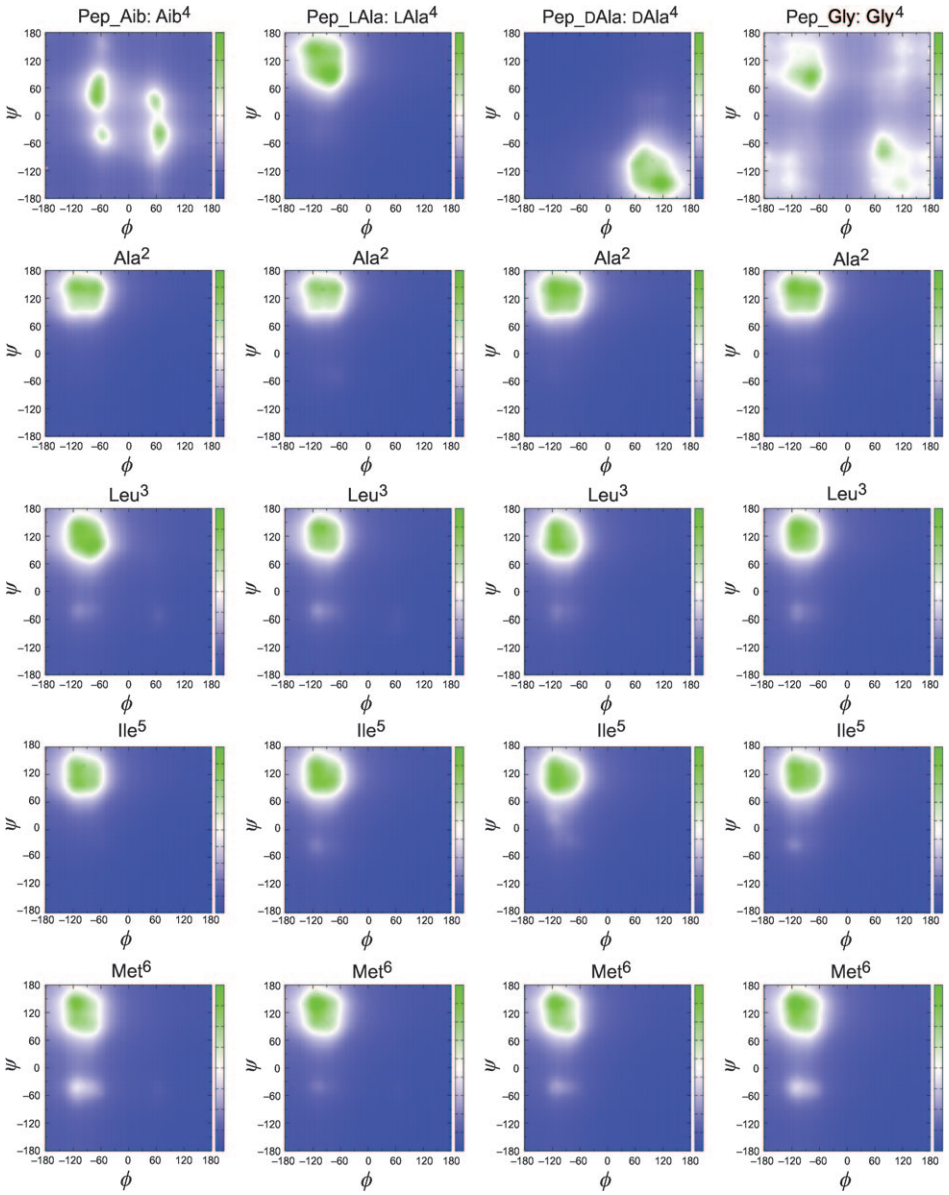

Fig. 11. Ramachandran *plots of Aib*[4], L-*Ala*[4], D-*Ala*[4], *or Gly*[4] (*Line 1*) *and Ala*[2], *Leu*[3], *Ile*[5], *and Met*[6] *in Pep_Aib* (*Column 1*), *in Pep_*L*Ala* (*Column 2*), *in Pep_*D*Ala* (*Column 3*), *and in Pep_Gly* (*Column 4*). The color scale represents the number of solute configurations in the trajectory, and the green color corresponds to the solute conformation that has the largest population.

study [45] in which a dipeptide containing an Aib residue was found to adopt many conformations in a nonpolar solvent. As proposed [45], the Aib residue displays the same conformational freedom as other amino acid residues do. In a recent combined

experimental and MD study of tripeptides in H_2O [20], the ϕ/ψ angles of the Aib residue were found to be confined to the regions of helical conformation. These studies indicate the substantial influence of the solvent on the folding behavior of an Aib residue in solution. Indeed, in simulations with different solvents, namely MeOH, DMSO, and H_2O, the four conformations were sampled with different populations (*Table 3*). DMSO has a higher polarity than MeOH and displays a slight preference for Helix^L when compared to MeOH. With H_2O as the solvent, the Helix^L is much more favored, while the population of the C_7 conformation decreases to 7%.

Table 3. *Populations* [%] *of Four Conformations*[a]) *of the Aib Residue in the Simulations of Pep_Aib in Different Solvents*

Solvent	ε[b])	Helix^L	Helix^R	C_7	C'_7
MeOH	18	7	11	26	17
DMSO[c])	46	12	13	17	20
H_2O[c])	61	21	14	7	22

[a]) The criterion used to distinguish the four conformations is: Helix^L: $40° \le \phi \le 80°$, $10° \le \psi \le 50°$; Helix^R: $-80° \le \phi \le -40°$, $-50° \le \psi \le -10°$; C_7: $-80° \le \phi \le -10°$, $10° \le \psi \le 80°$; C'_7: $10° \le \phi \le 80°$, $-80° \le \psi \le -10°$. [b]) Dielectric permittivity of the model solvents. [c]) Manuscript in preparation.

We note that in previous MD studies on Aib-rich peptides in both DMSO and MeOH carried out in our group [15–18], the Aib residue displays a rather narrow distribution in the regions of helical conformations in the *Ramachandran* map. This qualifies the application of the GROMOS force field to the folding and unfolding behavior of Aib-containing peptides in DMSO and MeOH. As shown in these studies, the Aib residue displays a higher propensity to induce $3_{10}/\alpha$ helical conformation in Aib-rich peptides. The reason that, in our present study, the Aib residue shows distributions not only in the helical region but also in the C7 region may be the low presence of Aib, one single Aib residue in the heptapeptide. The propensity to fold to a helix is increased with the appearance of several Aib residues in the peptide, either sequentially [15–17] or alternatively [18].

As the simplest amino acid, Gly is conformationally very flexible and less likely to contribute to the formation of helices, while it has a high occurrence in β-turns [1][58][59][61]. As seen in *Fig. 11*, the sampling of Gly has reached all four quadrants of the *Ramachandran* map.

4. Conclusion. – Through a QM study on a simplified model and a MD simulation study on a prototype α-heptapeptide and its three analogues in MeOH, we analyzed the propensity of a single Aib residue to induce helical conformation. The agreement of the simulated trajectories with the experimentally determined NOE atom–atom distance bounds and ^3J-coupling-constant values warrants a further interpretation of the obtained conformational ensembles.

In line with previous studies, our calculations indicate that the allowed region of conformational space for Aib is more narrow than for Ala and Gly. According to our calculations, in both the gas phase and MeOH solvent at 300 K, the Aib residue may

adopt either the C_7 or the helical conformation, in contrast to crystallographical studies. This is due to the different forces that are imposed on the peptides in crystalline states *vs.* the liquid phase. Previous studies, both experimental [63] and theoretical [64][65], have shown that proteins may adopt similar conformations in solution and in the crystalline state which is likely to be due to the high percentage of solvent content in protein crystals. This does not hold for crystals of small peptides, which contain only a limited number of solvent molecules or are even solvent-free, thus build a much different environment for the peptides. In these cases, the lattice forces in the crystalline state may be dominant and induce a different preference for a specific conformation, depending on the sequence of the peptide. In the α-heptapeptide under study, there is only one Aib residue, and the other six residues do not have a strong preference for the helical conformation. The low content of Aib residues in the peptide is not sufficient to induce a helix as the dominant form of the peptide in MeOH.

The folding of the peptide appears to be solvent-dependent. With an increase of the polarity of the solvent, the helical conformations become more accessible, while the C_7 conformation becomes less populated.

In summary, by means of a DFT study and a molecular-dynamics study based on the GROMOS force field, we are able to describe the propensity of an Aib residue to induce folding to a helix compared to that of Ala and Gly residues. The Aib residue has a stronger propensity to induce a helical secondary structure, while to generate a thermally stable helical conformation of a linear peptide, a high presence of Aib residues in the peptide is required.

The authors thank the *Swiss National Science Foundation* and its *National Competence Center for Research* (*NCCR*) *in Structural Biology* for financial support.

REFERENCES

[1] I. L. Karle, *Biopolymers* **2001**, *60*, 351.
[2] J. Venkatraman, S. C. Shankaramma, P. Balaram, *Chem. Rev.* **2001**, *101*, 3131.
[3] S. Aravinda, N. Shamala, R. S. Roy, P. Balaram, *Proc. Indian Acad. Sci. (Chem. Sci.)* **2003**, *115*, 373.
[4] S. Aravinda, N. Shamala, P. Balaram, *Chem. Biodiversity* **2008**, *5*, 1238.
[5] I. L. Karle, J. L. Flippen-Anderson, K. Uma, M. Sukumar, P. Balaram, *J. Am. Chem. Soc.* **1990**, *112*, 9350.
[6] A. K. Francis, M. Iqbal, P. Balaram, M. Vijayan, *FEBS Lett.* **1983**, *155*, 230.
[7] C. Toniolo, *Biopolymers* **1989**, *28*, 247.
[8] R. Gratias, R. Konat, H. Kessler, M. Crisma, G. Valle, A. Polese, F. Formaggio, C. Toniolo, Q. B. Broxterman, J. Kamphuis, *J. Am. Chem. Soc.* **1998**, *120*, 4763.
[9] K. Gunasekaran, 'Stereo-chemical Analysis of Protein Structures-Lessons for Design, Engineering and Prediction', Ph.D. Thesis, Indian Institute of Science, Bangalore, 1997.
[10] G. R. Marshall, H. E. Bosshard, *Circ. Res.* **1972**, *30*/*31*(suppl. II), 143.
[11] A. W. Burgess, S. J. Leach, *Biopolymers* **1973**, *12*, 2599.
[12] H. A. Scheraga, *Chem. Rev.* **1971**, *71*, 195.
[13] M. Mutter, S. Vuilleumier, *Angew. Chem., Int. Ed. Engl.* **1989**, *28*, 535.
[14] D. Seebach, B. Jaun, R. Sebesta, R. I. Mathad, O. Flögel, M. Limbach, H. Sellner, S. Cottens, *Helv. Chim. Acta* **2006**, *89*, 1801.
[15] M. Bellanda, E. Peggion, R. Bürgi, W. F. van Gunsteren, S. Mammi, *J. Pept. Res.* **2001**, *57*, 97.
[16] R. Bürgi, X. Daura, A. Mark, M. Bellanda, S. Mammi, E. Peggion, W. F. van Gunsteren, *J. Pept. Res.* **2001**, *57*, 107.

[17] H. Yu, M. Ramseier, R. Bürgi, W. F. van Gunsteren, *ChemPhysChem* **2004**, *5*, 633.
[18] D. Wang, B. Jaun, W. F. van Gunsteren, *ChemBioChem* **2009**, *10*, 2032.
[19] R. Bosch, G. Jung, K.-P. Voges, W. Winter, *Liebigs Ann. Chem.* **1984**, 1117.
[20] R. Schweitzer-Stenner, W. Gonzales, G. T. Bourne, J. A. Feng, G. R. Marshall, *J. Am. Chem. Soc.* **2007**, *129*, 13095.
[21] D. Seebach, R. I. Mathad, T. Kimmerlin, Y. R. Mahajan, P. Bindschädler, M. Rueping, B. Jaun, C. Hilty, T. Etezady-Esfarjani, *Helv. Chim. Acta* **2005**, *88*, 1969.
[22] D. Seebach, M. Overhand, F. N. M. Kühnle, B. Martinoni, L. Oberer, U. Hommel, H. Widmer, *Helv. Chim. Acta* **1996**, *79*, 913.
[23] D. Seebach, P. E. Ciceri, M. Overhand, B. Jaun, D. Rigo, L. Oberer, U. Hommel, R. Amstutz, H. Widmer, *Helv. Chim. Acta* **1996**, *79*, 2043.
[24] T. Soares, M. Christen, K. Hu, W. F. van Gunsteren, *Tetrahedron* **2004**, *60*, 7775.
[25] M. Karplus, J. A. McCammon, *Nat. Struct. Biol.* **2002**, *9*, 646; Corrigenda: *Nat. Struct. Biol.* **2002**, *9*, 788.
[26] W. F. van Gunsteren, D. Bakowies, R. Baron, I. Chandrasekhar, M. Christen, X. Daura, P. Gee, D. P. Geerke, A. Glättli, P. H. Hünenberger, M. A. Kastenholz, C. Oostenbrink, M. Schenk, D. Trzesniak, N. F. A. van der Vegt, H. B. Yu, *Angew. Chem*. **2006**, 118, 4168; *Angew. Chem., Int. Ed.* **2006**, *45*, 4064.
[27] S. A. Adcock, J. A. McCammon, *Chem. Rev.* **2006**, *106*, 1589.
[28] C. Oostenbrink, A. Villa, A. E. Mark, W. F. van Gunsteren, *J. Comput. Chem.* **2004**, *25*, 1656.
[29] R. Walser, A. E. Mark, W. F. van Gunsteren, M. Lauterbach, G. Wipff, *J. Chem. Phys.* **2000**, *112*, 10450.
[30] W. F. van Gunsteren, S. R. Billeter, A. A. Eising, P. H. Hünenberger, P. Krüger, A. E. Mark, W. R. P. Scott, I. G. Tironi, 'Biomolecular Simulation: The GROMOS96 Manual and User Guide', vdf Hochschulverlag, ETH Zürich, 1996.
[31] W. R. P. Scott, P. H. Hünenberger, I. G. Tironi, A. E. Mark, S. R. Billeter, J. Fennen, A. E. Torda, T. Huber, P. Krüger, W. F. van Gunsteren, *J. Phys. Chem.* **1999**, *103*, 3596.
[32] J.-P. Ryckaert, G. Ciccotti, H. J. C. Berendsen, *J. Comput. Phys.* **1977**, *23*, 327.
[33] J. A. Barker, R. O. Watts, *Mol. Phys.* **1973**, *26*, 789.
[34] I. G. Tironi, R. Sperb, P. E. Smith, W. F. van Gunsteren, *J. Chem. Phys.* **1995**, *102*, 5451.
[35] H. J. C. Berendsen, J. P. M. Postma, W. F. van Gunsteren, A. DiNola, J. R. Haak, *J. Chem. Phys.* **1984**, *81*, 3684.
[36] Z. Gattin, A. Glättli, B. Jaun, W. F. van Gunsteren, *Biopolymers* **2007**, *85*, 318.
[37] X. Daura, W. F. van Gunsteren, A. E. Mark, *Proteins* **1999**, *34*, 269.
[38] K. Wüthrich, M. Billeter, W. Braun, *J. Mol. Biol.* **1983**, *169*, 949.
[39] M. Karplus, *J. Chem. Phys.* **1959**, *30*, 11.
[40] M. Karplus, *J. Am. Chem. Soc.* **1963**, *85*, 2870.
[41] A. Pardi, M. Billeter, K. Wüthrich, *J. Mol. Biol.* **1984**, *180*, 741.
[42] D. P. Geerke, C. Oostenbrink, N. F. A. van der Vegt, W. F. van Gunsteren, *J. Phys. Chem. B* **2004**, *108*, 1436.
[43] H. J. C. Berendsen, J. P. M. Postma, W. F. van Gunsteren, J. Hermans, 'Interaction Models for Water in Relation to Protein Hydration', in 'Intermolecular Forces', Ed. B. Pullman, Reidel Dordrecht, The Netherlands, 1981, pp. 331 – 342.
[44] T. N. Heinz, W. F. van Gunsteren, P. H. Hünenberger, *J. Chem. Phys.* **2001**, *115*, 1125.
[45] A. Aubry, J. Protas, G. Boussard, M. Marraud, J. Neel, *Biopolymers* **1978**, *17*, 1693.
[46] V. Barone, F. Fraternali, P. L. Cristinziano, *Macromolecules* **1990**, *23*, 2038.
[47] C. Alemán, J. J. Perez, *Int. J. Quantum Chem.* **1993**, *47*, 231.
[48] C. Aleman, J. Casanovas, *J. Chem. Soc., Perkin Trans. 2* **1994**, 563.
[49] A. D. Becke, *J. Chem. Phys.* **1993**, *98*, 5648.
[50] C. Lee, W. Yang, R. G. Parr, *Phys. Rev. B* **1988**, *37*, 785.
[51] W. J. Hehre, R. Ditchfield, J. A. Pople, *J. Chem. Phys.* **1972**, *56*, 2257.
[52] S. F. Sousa, P. A. Fernandes, M. J. Ramos, *J. Phys. Chem. A* **2007**, *111*, 10439.
[53] L. Rao, H. Ke, G. Fu, X. Xu, Y. Yan, *J. Chem. Theory Comput.* **2009**, *5*, 86.

[54] M. J. Frisch, G. W. Trucks, H. B. Schlegel, G. E. Scuseria, M. A. Robb, J. R. Cheeseman, J. A. Montgomery Jr., T. Vreven, K. N. Kudin, J. C. Burant, J. M. Millam, S. S. Iyengar, J. Tomasi, V. Barone, B. Mennucci, M. Cossi, G. Scalmani, N. Rega, G. A. Petersson, H. Nakatsuji, M. Hada, M. Ehara, K. Toyota, R. Fukuda, J. Hasegawa, M. Ishida, T. Nakajima, Y. Honda, O. Kitao, H. Nakai, M. Klene, X. Li, J. E. Knox, H. P. Hratchian, J. B. Cross, V. Bakken, C. Adamo, J. Jaramillo, R. Gomperts, R. E. Stratmann, O. Yazyev, A. J. Austin, R. Cammi, C. Pomelli, J. W. Ochterski, P. Y. Ayala, K. Morokuma, G. A. Voth, P. Salvador, J. J. Dannenberg, V. G. Zakrzewski, S. Dapprich, A. D. Daniels, M. C. Strain, O. Farkas, D. K. Malick, A. D. Rabuck, K. Raghavachari, J. B. Foresman, J. V. Ortiz, Q. Cui, A. G. Baboul, S. Clifford, J. Cioslowski, B. B. Stefanov, G. Liu, A. Liashenko, P. Piskorz, I. Komaromi, R. L. Martin, D. J. Fox, T. Keith, M. A. Al-Laham, C. Y. Peng, A. Nanayakkara, M. Challacombe, P. M. W. Gill, B. Johnson, W. Chen, M. W. Wong, C. Gonzalez, J. A. Pople, Gaussian 03, Revision D.01, Gaussian Inc., Wallingford CT, 2004.
[55] M. Tsai, Y. Xu, J. J. Dannenberg, *J. Phys. Chem. B* **2009**, *113*, 309.
[56] D. Trzesniak, A. Glättli, B. Jaun, W. F. van Gunsteren, *J. Am. Chem. Soc.* **2005**, *127*, 14320.
[57] B. V. V. Prasad, P. Balaram, *CRC Crit. Rev. Biochem.* **1984**, *16*, 307.
[58] J. S. Richardson, *Adv. Protein Chem.* **1981**, *34*, 167.
[59] C. Ramakrishnan, N. Srinivasan, *Curr. Sci.* **1990**, *59*, 851.
[60] B. L. Sibanda, J. M. Thornton, *Nature (London)* **1985**, *316*, 170.
[61] C. M. Wilmot, J. M. Thornton, *J. Mol. Biol.* **1988**, *20*, 221.
[62] B. L. Sibanda, T. L. Blundell, J. M. Thornton, *J. Mol. Biol.* **1989**, *206*, 759.
[63] M. Billeter, A. D. Kline, W. Braun, R. Huber, K. Wüthrich, *J. Mol. Biol.* **1989**, *206*, 677.
[64] W. F. van Gunsteren, H. J. C. Berendsen, *J. Mol. Biol.* **1984**, *176*, 559.
[65] U. Stocker, K. Spiegel, W. F. van Gunsteren, *J. Biomol. NMR* **2000**, *18*, 1.

Received November 27, 2009